Optimal and Suboptimal Finger Selection Algorithms for MMSE Rake Receivers in Impulse Radio Ultra-Wideband Systems[1]

Sinan Gezici, Mung Chiang, H. Vincent Poor and Hisashi Kobayashi
Department of Electrical Engineering
Princeton University, Princeton, NJ 08544
{sgezici,chiangm,poor,hisashi}@princeton.edu

***Abstract*— Convex relaxations of the optimal finger selection algorithm are proposed for a minimum mean square error (MMSE) Rake receiver in an impulse radio ultra-wideband system. First, the optimal finger selection problem is formulated as an integer programming problem with a non-convex objective function. Then, the objective function is approximated by a convex function and the integer programming problem is solved by means of constraint relaxation techniques. The proposed algorithms are suboptimal due to the approximate objective function and the constraint relaxation steps. However, they can be used in conjunction with the conventional finger selection algorithm, which is suboptimal on its own since it ignores the correlation between multipath components, to obtain performances reasonably close to that of the optimal scheme that cannot be implemented in practice due to its complexity. The proposed algorithms leverage convexity of the optimization problem formulations, which is the watershed between 'easy' and 'difficult' optimization problems.**

***Index Terms*— Ultra-wideband (UWB), impulse radio (IR), MMSE Rake receiver, convex optimization, integer programming.**

I. INTRODUCTION

Since the US Federal Communications Commission (FCC) approved the limited use of ultra-wideband (UWB) technology [1], communications systems that employ UWB signals have drawn considerable attention. A UWB signal is defined to be one that possesses an absolute bandwidth larger than 500MHz or a relative bandwidth larger than 20% and can coexist with incumbent systems in the same frequency range due to its large spreading factor and low power spectral density. UWB technology holds great promise for a variety of applications such as short-range high-speed data transmission and precise location estimation.

Commonly, impulse radio (IR) systems, which transmit very short pulses with a low duty cycle, are employed to implement UWB systems ([2]-[6]). In an IR system, a train of pulses is sent and information is usually conveyed by the position or the polarity of the pulses, which correspond to Pulse Position Modulation (PPM) and Binary Phase Shift Keying (BPSK), respectively. In order to prevent catastrophic collisions among different users and thus provide robustness against multiple-access interference, each information symbol is represented by a sequence of pulses; the positions of the pulses within that sequence are determined by a pseudo-random time-hopping (TH) sequence specific to each user [2]. The number N_f of pulses representing one information symbol can also be interpreted as pulse combining gain.

Commonly, users in an IR-UWB system employ Rake receivers to collect energy from different multipath components. A Rake receiver combining all the paths of the incoming signal is called an *all-Rake* (*ARake*) receiver. Since a UWB signal has a very wide bandwidth, the number of resolvable multipath components is usually very large. Hence, an ARake receiver is not implemented in practice due to its complexity. However, it serves as a benchmark for the performance of more practical Rake receivers. A feasible implementation of multipath diversity combining can be obtained by a *selective-Rake* (*SRake*) receiver, which combines the M best, out of L, multipath components [7]. Those M best components are determined by a finger selection algorithm. For a maximal ratio combining (MRC) Rake receiver, the paths with highest signal-to-noise ratios (SNRs) are selected, which is an optimal scheme in the absence of interfering users and inter-symbol interference (ISI). For a minimum mean square error (MMSE) Rake receiver, the "conventional" finger selection algorithm is to choose the paths with highest signal-to-interference-plus-noise ratios (SINRs). This conventional scheme is not necessarily optimal since it ignores the correlation of the noise terms at different multipath components. In other words, choosing the paths with highest SINRs does not necessarily maximizes the overall SINR of the system.

In this paper, we formulate the optimal MMSE SRake as a nonconvex, integer-constrained optimization, where the aim is to choose the finger locations of the receiver so as to maximize the overall SINR. While computing the optimal finger selection is NP-hard, we present several relaxation methods to turn the (approximate) problem into convex optimization problems that can be very efficiently solved by interior-point methods, which are polynomial time in the worst case, and very fast in practice. These optimal finger selection relaxations produce significantly higher average SINR than the conventional one that ignores the correlations, and represent a numerically efficient way to strike a balance between SINR optimality and computational tractability.

The remainder of the paper is organized as follows. Sec-

[1]This research is supported in part by the National Science Foundation under grants ANI-03-38807, CNS-0417603, and CCR-0440443, and in part by the New Jersey Center for Wireless Telecommunications.

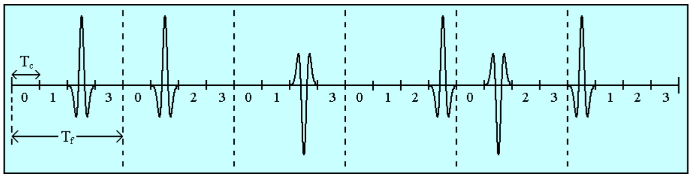

Fig. 1. An example time-hopping impulse radio signal with pulse-based polarity randomization, where $N_f = 6$, $N_c = 4$, the time hopping sequence is {2,1,2,3,1,0} and the polarity codes are {+1,+1,-1,+1,-1,+1}.

tion II describes the transmitted and received signal models in a multiuser frequency-selective environment. The finger selection problem is formulated and the optimal algorithm is described in Section III, which is followed by a brief description of the conventional algorithm in Section IV. In Section V, two convex relaxations of the optimal finger selection algorithm, based on an approximate SINR expression and integer constraint relaxation techniques, are proposed. The simulation results are presented in Section VI, and the concluding remarks are made in the last section.

II. Signal Model

We consider a synchronous, binary phase shift keyed TH-IR system with K users, in which the transmitted signal from user k is represented by:

$$s_{tx}^{(k)}(t) = \sqrt{\frac{E_k}{N_f}} \sum_{j=-\infty}^{\infty} d_j^{(k)}\, b_{\lfloor j/N_f \rfloor}^{(k)} p_{tx}(t - jT_f - c_j^{(k)} T_c), \tag{1}$$

where $p_{tx}(t)$ is the transmitted UWB pulse, E_k is the bit energy of user k, T_f is the "frame" time, N_f is the number of pulses representing one information symbol, and $b_{\lfloor j/N_f \rfloor}^{(k)} \in \{+1, -1\}$ is the binary information symbol transmitted by user k. In order to allow the channel to be shared by many users and avoid catastrophic collisions, a time-hopping (TH) sequence $\{c_j^{(k)}\}$, where $c_j^{(k)} \in \{0, 1, ..., N_c - 1\}$, is assigned to each user. This TH sequence provides an additional time shift of $c_j^{(k)} T_c$ seconds to the jth pulse of the kth user where T_c is the chip interval and is chosen to satisfy $T_c \leq T_f/N_c$ in order to prevent the pulses from overlapping. We assume $T_f = N_c T_c$ without loss of generality. The random polarity codes $d_j^{(k)}$ are binary random variables taking values ± 1 with equal probability ([8]-[10]).

Consider the discrete presentation of the channel, $\boldsymbol{\alpha}^{(k)} = [\alpha_1^{(k)} \cdots \alpha_L^{(k)}]$ for user k, where L is assumed to be the number of multipath components for each user, and T_c is the multipath resolution. Then, the received signal can be expressed as

$$r(t) = \sum_{k=1}^{K} \sqrt{\frac{E_k}{N_f}} \sum_{j=-\infty}^{\infty} \sum_{l=1}^{L} \alpha_l^{(k)} d_j^{(k)}\, b_{\lfloor j/N_f \rfloor}^{(k)} \times p_{rx}(t - jT_f - c_j^{(k)} T_c - (l-1)T_c) + \sigma_n n(t), \tag{2}$$

where $p_{rx}(t)$ is the received unit-energy UWB pulse, which is usually modelled as the derivative of $p_{tx}(t)$ due to the effects

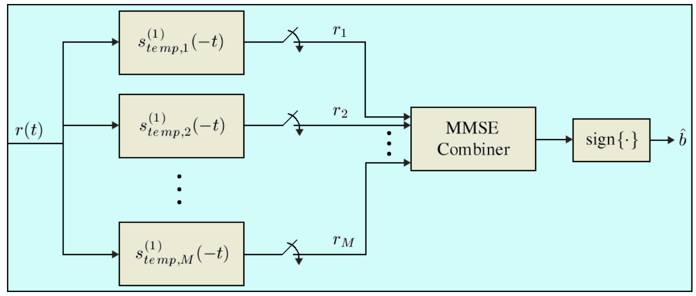

Fig. 2. The receiver structure. There are M multipath components, which are combined by the MMSE combiner.

of the antenna, and $n(t)$ is zero mean white Gaussian noise with unit spectral density.

We assume that the time-hopping sequence is constrained to the set $\{0, 1, \ldots, N_T - 1\}$, where $N_T \leq N_c - L$, so that there is no inter-frame interference (IFI).

Due to the high resolution of UWB signals, chip-rate and frame rate sampling are not very practical for such systems. In order to have a lower sampling rate, the received signal can be correlated with template signals which enable symbol rate sampling of the output [11]. The template signal for the lth path of the incoming signal can be expressed as

$$s_{temp,l}^{(1)}(t) = \sum_{j=iN_f}^{(i+1)N_f - 1} d_j^{(1)}\, p_{rx}(t - jT_f - c_j^{(1)} T_c - (l-1)T_c), \tag{3}$$

for the ith information symbol, where we consider user 1 without loss of generality. In other words, by using a correlator for each multipath component that we want to combine, we can just use symbol rate sampling at each branch, as shown in Figure 2.

Note that the use of such template signals results in equal gain combining (EGC) of different frame components. This may not be optimal under some conditions (see [12] for (sub)optimal schemes). However, it is very practical since it facilitates symbol-rate sampling. Since we consider a system that employs template signals of the form (3), i.e. EGC of frame components, it is sufficient to consider the problem of selection of the optimal paths just for one frame. Hence, we assume $N_f = 1$ without loss of generality.

Let $\mathcal{L} = \{l_1, \ldots, l_M\}$ denote the set of multipath components that the receiver collects (Figure 2). At each branch, the signal is effectively passed through a matched filter (MF) matched to the related template signal in (3) and sampled once for each symbol. Then, the discrete signal for the lth path can be expressed, for the ith information symbol, as[2]

$$r_l = \mathbf{s}_l^T \mathbf{A} \mathbf{b}_i + n_l, \tag{4}$$

for $l = l_1, \ldots, l_M$, where $\mathbf{A} = \text{diag}\{\sqrt{E_1}, \ldots, \sqrt{E_K}\}$, $\mathbf{b}_i = [b_i^{(1)} \cdots b_i^{(K)}]^T$ and $n_l \sim \mathcal{N}(0, \sigma_n^2)$. $\mathbf{s}_l$ is a $K \times 1$ vector,

[2]Note that the dependence of r_l on the index of the information symbol, i, is not shown explicitly.

which can be expressed as a sum of the desired signal part (SP) and multiple-access interference (MAI) terms:

$$\mathbf{s}_l = \mathbf{s}_l^{(SP)} + \mathbf{s}_l^{(MAI)}, \tag{5}$$

where the kth elements can be expressed as

$$\left[\mathbf{s}_l^{(SP)}\right]_k = \begin{cases} \alpha_l^{(1)}, & k = 1 \\ 0, & k = 2, \ldots, K \end{cases} \quad \text{and} \tag{6}$$

$$\left[\mathbf{s}_l^{(MAI)}\right]_k = \begin{cases} 0, & k = 1 \\ d_1^{(1)} d_1^{(k)} \sum_{m=1}^{L} \alpha_m^{(k)} I_{l,m}^{(k)}, & k = 2, \ldots, K \end{cases}, \tag{7}$$

with $I_{l,m}^{(k)}$ being the indicator function that is equal to 1 if the mth path of user k collides with the lth path of user 1, and 0 otherwise.

III. Problem Formulation and Optimal Solution

The problem is to choose the optimal set of multipath components, $\mathcal{L} = \{l_1, \ldots, l_M\}$, that minimizes the bit error probability (BEP) of the system. In other words, we need to choose the best samples from the L received samples r_l, $l = 1, \ldots, L$, as shown in (4).

To reformulate this combinatorial problem, we first define an $M \times L$ selection matrix $\mathbf{X}$ as follows: M of the columns of $\mathbf{X}$ are the unit vectors $\mathbf{e}_1, \ldots, \mathbf{e}_M$ ($\mathbf{e}_i$ having a 1 at its ith position and zero elements for all other entries), and the other columns are all zero vectors. The column indices of the unit vectors determine the subset of the multipath components that are selected. For example, for $L = 4$ and $M = 2$, $\mathbf{X} = \begin{bmatrix} 0 & 1 & 0 & 0 \\ 0 & 0 & 1 & 0 \end{bmatrix}$ chooses the second and third multipath components.

Using the selection matrix $\mathbf{X}$, we can express the vector of received samples from M multipath components as

$$\mathbf{r} = \mathbf{XSAb}_i + \mathbf{Xn}, \tag{8}$$

where $\mathbf{n}$ is the vector of thermal noise components $\mathbf{n} = [n_1 \cdots n_L]^T$, and $\mathbf{S}$ is the signature matrix given by $\mathbf{S} = [\mathbf{s}_1 \cdots \mathbf{s}_L]^T$, with $\mathbf{s}_l$ as in (5).

Using (5)-(7), (8) can be expressed as

$$\mathbf{r} = b_i^{(1)} \sqrt{E_1} \mathbf{X} \boldsymbol{\alpha}^{(1)} + \mathbf{XS}^{(MAI)} \mathbf{Ab}_i + \mathbf{Xn}, \tag{9}$$

where $\mathbf{S}^{(MAI)}$ is the MAI part of the signature matrix $\mathbf{S}$.

Then, the linear MMSE receiver can be expressed as

$$\hat{b}_i = \text{sign}\{\boldsymbol{\theta}^T \mathbf{r}\}, \tag{10}$$

where the MMSE weight vector is given by [13]

$$\boldsymbol{\theta} = \mathbf{R}^{-1} \mathbf{X} \boldsymbol{\alpha}^{(1)}, \tag{11}$$

with $\mathbf{R}$ being the correlation matrix of the noise term:

$$\mathbf{R} = \mathbf{XS}^{(MAI)} \mathbf{A}^2 (\mathbf{S}^{(MAI)})^T \mathbf{X}^T + \sigma_n^2 \mathbf{I}. \tag{12}$$

The SINR of the system can be expressed as

$$SINR(\mathbf{X}) = \frac{E_1}{\sigma_n^2} (\boldsymbol{\alpha}^{(1)})^T \mathbf{X}^T \times \left(\mathbf{I} + \frac{1}{\sigma_n^2} \mathbf{XS}^{(MAI)} \mathbf{A}^2 (\mathbf{S}^{(MAI)})^T \mathbf{X}^T \right)^{-1} \mathbf{X} \boldsymbol{\alpha}^{(1)}. \tag{13}$$

Hence, the optimal path/finger selection problem can be formulated as

$$\text{maximize } SINR(\mathbf{X}), \tag{14}$$

where $\mathbf{X}$ has the previously defined structure.

Note that the objective function to be maximized is not concave and the optimization variable $\mathbf{X}$ takes binary values, with the previously defined structure. In other words, two major difficulties arise in solving (14) globally: nonconvex optimization and integer constraints. Either makes the problem NP-hard. Therefore, it is an intractable optimization problem in this general form.

IV. Conventional Algorithm

Instead of the solving the problem in (14), the "conventional" finger selection algorithm chooses the M paths with largest individual SINRs, where the SINR for the lth path can be expressed as

$$SINR_l = \frac{E_1 (\alpha_l^{(1)})^2}{(\mathbf{s}_l^{(MAI)})^T \mathbf{A}^2 \mathbf{s}_l^{(MAI)} + \sigma_n^2}, \tag{15}$$

for $l = 1, \ldots, L$.

This algorithm is not optimal because it ignores the correlation of the noise components of different paths. Therefore, it does not always maximize the overall SINR of the system given in (13). For example, the contribution of two highly correlated strong paths to the overall SINR might be worse than the contribution of one strong and one relatively weaker, but uncorrelated, paths. The correlation between the multipath components is the result of the MAI from the other users in the system.

V. Relaxations of Optimal Finger Selection

Since the optimal solution in (14) is quite difficult, we first consider an approximation of the objective function in (13). When the eigenvalues of $\frac{1}{\sigma_n^2} \mathbf{XS}^{(MAI)} \mathbf{A}^2 (\mathbf{S}^{(MAI)})^T \mathbf{X}^T$ are considerably smaller than 1, which occurs when the MAI is not very strong compared to the thermal noise, we can approximate the SINR expression in (13) as follows[3]:

$$SINR(\mathbf{X}) \approx \frac{E_1}{\sigma_n^2} (\boldsymbol{\alpha}^{(1)})^T \mathbf{X}^T \times \left(\mathbf{I} - \frac{1}{\sigma_n^2} \mathbf{XS}^{(MAI)} \mathbf{A}^2 (\mathbf{S}^{(MAI)})^T \mathbf{X}^T \right) \mathbf{X} \boldsymbol{\alpha}^{(1)}, \tag{16}$$

[3]More accurate approximations can be obtained by using higher order series expansions for the matrix inverse in (13). However, the solution of the optimization problem does not lend itself to low complexity solutions in those cases.

which can be expressed as

$$SINR(\mathbf{X}) \approx \frac{E_1}{\sigma_n^2}\{\,(\boldsymbol{\alpha}^{(1)})^T\mathbf{X}^T\mathbf{X}\boldsymbol{\alpha}^{(1)} - \frac{1}{\sigma_n^2}\boldsymbol{\alpha}^{(1)}\mathbf{X}^T\mathbf{X}\mathbf{S}^{(MAI)}\mathbf{A}^2(\mathbf{S}^{(MAI)})^T\mathbf{X}^T\mathbf{X}\boldsymbol{\alpha}^{(1)}\,\}. \quad (17)$$

Note that the approximate $SINR$ expression depends on $\mathbf{X}$ only through $\mathbf{X}^T\mathbf{X}$. Defining $\mathbf{x} = [x_1 \cdots x_L]^T$ as the diagonal elements of $\mathbf{X}^T\mathbf{X}$, $\mathbf{x} = \text{diag}\{\mathbf{X}^T\mathbf{X}\}$, we have $x_i = 1$ if the ith path is selected, and $x_i = 0$ otherwise; and $\sum_{i=1}^{L} x_i = M$. Then, we obtain, after some manipulation,

$$SINR(\mathbf{x}) = \frac{E_1}{\sigma_n^2}\left\{\mathbf{q}^T\mathbf{x} - \frac{1}{\sigma_n^2}\mathbf{x}^T\mathbf{P}\mathbf{x}\right\}, \quad (18)$$

where $\mathbf{q} = [(\alpha_1^{(1)})^2 \cdots (\alpha_L^{(1)})^2]^T$ and $\mathbf{P} = \text{diag}\{\alpha_1^{(1)} \cdots \alpha_L^{(1)}\}\mathbf{S}^{(MAI)}\mathbf{A}^2(\mathbf{S}^{(MAI)})^T\text{diag}\{\alpha_1^{(1)} \cdots \alpha_L^{(1)}\}$.

Then, we can formulate the finger selection problem as follows:

$$\begin{aligned} \text{minimize} \quad & \frac{1}{\sigma_n^2}\mathbf{x}^T\mathbf{P}\mathbf{x} - \mathbf{x}^T\mathbf{q} \\ \text{subject to} \quad & \mathbf{x}^T\mathbf{1} = M, \\ & x_i \in \{0,1\}, \quad i = 1,\ldots,L. \end{aligned} \quad (19)$$

Note that the objective function is convex since $\mathbf{P}$ is positive definite, and that the first constraint is linear. However, the integer constraint increases the complexity of the problem. The common way to approximate the solution of an integer constraint problem is to use *constraint relaxation*. Then, the optimizer will be a continuous value instead of being binary and the problem (19) will be convex. Over the past decade, both powerful theory and efficient numerical algorithms have been developed for nonlinear convex optimization. It is now recognized that the watershed between "easy" and "difficult" optimization problems is not linearity but convexity. For example, the interior-point algorithms for nonlinear convex optimization are highly efficient, both in worst case complexity (provably polynomial time) and in practice (very fast even for a large number variables and constraints) [14]. Interior-point methods solve convex optimization problems with inequality constraints by applying Newton's method to a sequence of equality constrained problems, where the Newton's method is a kind of descent algorithm with the descent direction given by the Newton step [14].

We consider two different relaxation techniques in the following subsections.

A. Case-1: Relaxation to Sphere

Consider the relaxation of the integer constraint in (19) to a sphere that passes through all possible integer values. Then, the relaxed problem becomes

$$\begin{aligned} \text{minimize} \quad & \frac{1}{\sigma_n^2}\mathbf{x}^T\mathbf{P}\mathbf{x} - \mathbf{x}^T\mathbf{q} \\ \text{subject to} \quad & \mathbf{x}^T\mathbf{1} = M, \\ & (2\mathbf{x}-\mathbf{1})^T(2\mathbf{x}-\mathbf{1}) \leq L. \end{aligned} \quad (20)$$

Note that the problem becomes a convex quadratically constrained quadratic programming (QCQP) [14]. Hence it can be solved for global optimality using interior-point algorithms in polynomial time.

B. Case-2: Relaxation to Hypercube

As an alternative approach, we can relax the integer constraint in (19) to a hypercube constraint and get

$$\begin{aligned} \text{minimize} \quad & \frac{1}{\sigma_n^2}\mathbf{x}^T\mathbf{P}\mathbf{x} - \mathbf{x}^T\mathbf{q} \\ \text{subject to} \quad & \mathbf{x}^T\mathbf{1} = M, \\ & \mathbf{x} \in [0,1]^L, \end{aligned} \quad (21)$$

where the hypercube constraint can be expressed as $\mathbf{x} \succeq \mathbf{0}$ and $\mathbf{x} \preceq \mathbf{1}$, with $\mathbf{y} \succeq \mathbf{z}$ meaning that $y_1 \geq z_1, \ldots, y_L \geq z_L$. Note that the problem is now a linearly constrained quadratic programming (LCQP), and can be solved by interior-point algorithms [14] for the optimizer $\mathbf{x}^*$.

C. Dual Methods

We can also consider the dual problems. For the relaxation to the sphere considered in Section V-A, the Lagrangian for (20) can be obtained as

$$\mathcal{L}(\mathbf{x},\lambda,\nu) = \mathbf{x}^T\left(\frac{1}{\sigma_n^2}\mathbf{P} + 4\nu\mathbf{I}\right)\mathbf{x} - \mathbf{x}^T(\mathbf{q} - \lambda\mathbf{1} + 4\nu\mathbf{1}) - M\lambda, \quad (22)$$

where $\lambda \in \mathcal{R}$ and $\nu \in \mathcal{R}^+$.

After some manipulation, the Lagrange dual function can be expressed as

$$g(\lambda,\nu) = -\frac{1}{4}\left[\mathbf{q} + (\lambda+4\nu)\mathbf{1}\right]^T\left(\frac{1}{\sigma_n^2}\mathbf{P} + 4\nu\mathbf{I}\right)^{-1} \left[\mathbf{q} + (\lambda+4\nu)\mathbf{1}\right] - M\lambda, \quad (23)$$

Then, the dual problem becomes

minimize

$$\frac{1}{4}[\mathbf{q} + (\lambda+4\nu)\mathbf{1}]^T\left(\frac{1}{\sigma_n^2}\mathbf{P} + 4\nu\mathbf{I}\right)^{-1}[\mathbf{q} + (\lambda+4\nu)\mathbf{1}] + M\lambda \quad (24)$$

subject to $\quad \nu \geq 0, \quad (25)$

which can be solved for optimal λ and ν by interior point methods. Or, more simply, the unconstraint problem (24) can be solved using gradient descent algorithm, and then the optimizer $\bar{\nu}$ is mapped to $\nu^* = \max\{0, \bar{\nu}\}$.

After solving for optimal λ and μ, the optimizer $\mathbf{x}^*$ is obtained as

$$\mathbf{x}^* = \frac{1}{2}\left(\frac{1}{\sigma_n^2}\mathbf{P} + 4\nu^*\mathbf{I}\right)^{-1}[\mathbf{q} + (\lambda^* + 4\nu^*)\mathbf{1}]. \quad (26)$$

Note that the dual problem (24) has two variables, λ and ν, to optimize, compared to L variables, the components of $\mathbf{x}$, in the primal problem (20). However, an $L \times L$ matrix needs to be inverted for each iteration of the optimization of (24). Therefore, the primal problem can be preferred over the dual problem in this case.

Similarly, the dual problem for the relaxation in Section V-B can be obtained from (21) as

$$\text{minimize} \quad \frac{\sigma_n^2}{4}(\mathbf{q}+\boldsymbol{\mu}-\boldsymbol{\nu}-\lambda\mathbf{1})^T\mathbf{P}^{-1}(\mathbf{q}+\boldsymbol{\mu}-\boldsymbol{\nu}-\lambda\mathbf{1})+M\lambda+\boldsymbol{\nu}^T\mathbf{1} \tag{27}$$

$$\text{subject to} \quad \boldsymbol{\mu},\boldsymbol{\nu}\succeq\mathbf{0}. \tag{28}$$

It is observed from (27) that there are $2L+1$ variables and also $L\times L$ matrix inversion operations for the solution of the dual problem. Therefore, the simpler primal problem (21) is considered in the simulations.

D. Selection of Finger Locations

After solving the approximate problem (19) by means of integer relaxation techniques mentioned above, the finger location estimations are obtained by the indices of the M largest elements of the optimizer $\mathbf{x}^*$.

Both the approximation of the SINR expression by (16) and the integer relaxation steps result in the suboptimality of the solution. Therefore, it may not be very close to the optimal solution in some cases. However, it is expected to perform better than the conventional algorithm most of the time, since it considers the correlation between the multipath components. However, it is not guaranteed that the algorithms based on the convex relaxations of optimal finger selection always beat the conventional one. Since the conventional algorithm is very easy to implement, we can consider a hybrid algorithm where the final estimate of the convex relaxation algorithm is compared with that of the conventional one and the one that minimizes the exact SINR expression in (13) is chosen as the final estimate. In this way, the resulting hybrid suboptimal algorithm can get closer to the optimal solution.

VI. Simulation Results

The simulation results are performed to evaluate the performance of different finger selection algorithms for an IR-UWB system with $N_c = 20$ and $N_f = 1$. There are 5 equal energy users in the system ($K = 5$) and the users' TH and polarity codes are randomly generated. We model the channel coefficients as $\alpha_l = \text{sign}(\alpha_l)|\alpha_l|$ for $l = 1,\ldots,L$, where $\text{sign}(\alpha_l)$ is ±1 with equal probability and $|\alpha_l|$ is distributed lognormally as $\mathcal{LN}(\mu_l,\sigma^2)$. Also the energy of the taps is exponentially decaying as $\text{E}\{|\alpha_l|^2\} = \Omega_0 e^{-\lambda(l-1)}$, where λ is the decay factor and $\sum_{l=1}^{L}\text{E}\{|\alpha_l|^2\} = 1$ (so $\Omega_0 = (1-e^{-\lambda})/(1-e^{-\lambda L})$). For the channel parameters, we have $\lambda = 0.1$, $\sigma^2 = 0.5$ and μ_l can be calculated from $\mu_l = 0.5\left[\ln(\frac{1-e^{-\lambda}}{1-e^{-\lambda L}}) - \lambda(l-1) - 2\sigma^2\right]$, for $l = 1,\ldots,L$. We average the overall SINR of the system over different realizations of channel coefficients, TH and polarity codes of the users.

In Figure 3, we plot the average SINR of the system for different noise variances when $M = 5$ fingers are to be chosen out of $L = 15$ multipath components. As is observed from the figure, the convex relaxations of optimal finger selection result in SINR values reasonable close to those of the optimal

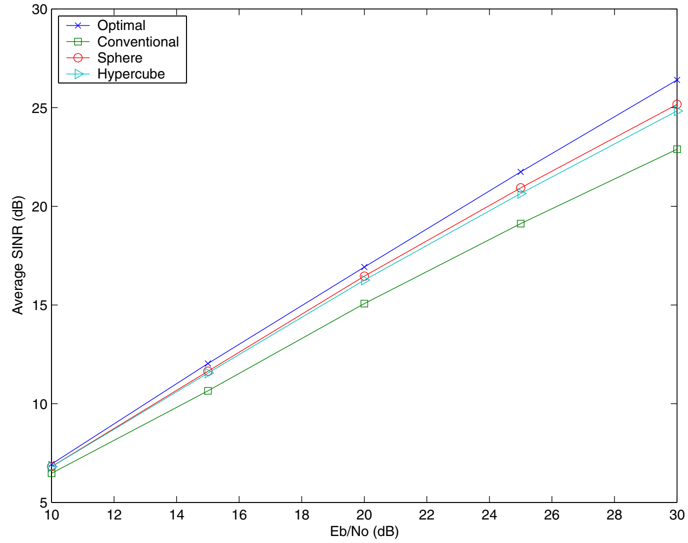

Fig. 3. Average SINR versus E_b/N_0 for $M = 5$ fingers. The channel has $L = 15$ multipath components and the taps are exponentially decaying. The IR-UWB system has $N_c = 20$ chips per frame and $N_f = 1$ frame per symbol. There are 5 equal energy users in the system and random TH and polarity codes are used.

exhaustive search scheme. Note that the gain by using the proposed algorithms over the conventional one increases as the thermal noise decreases. This is because when the thermal noise get less significant, the MAI becomes dominant, and the conventional technique gets worse since it ignores the correlation between the MAI noise terms when choosing the fingers.

Next, we plot SINR of the proposed suboptimal and conventional techniques for different finger numbers in Figure 4, where there are 50 multipath components and $E_b/N_0 = 20$. The number of chips per frame, N_c, is set to 75, and all other parameters are kept the same. In this case, the optimal algorithm takes a very long time to simulate since it needs to perform exhaustive search over many different finger combinations (therefore not implemented). The improvement using convex relaxations of optimal finger selection over the conventional technique decreases as M gets large since the channel is exponentially decaying and the most of the significant multipath components are already combined by all the algorithms.

Finally, we consider a MAI-limited scenario, where there are 10 users with $E_1 = 1$ and $E_k = 10\ \forall k$, and all the parameters are as in the previous case. Then, as shown in Figure 5, the improvement by using the suboptimal finger selection algorithms increase significantly. The main reason for this is that the suboptimal algorithms consider, although approximately, the correlation caused by MAI whereas the conventional scheme simply ignores that.

VII. Concluding Remarks

Optimal and suboptimal finger selection algorithms for MMSE-SRake receivers in an IR-UWB system are consid-

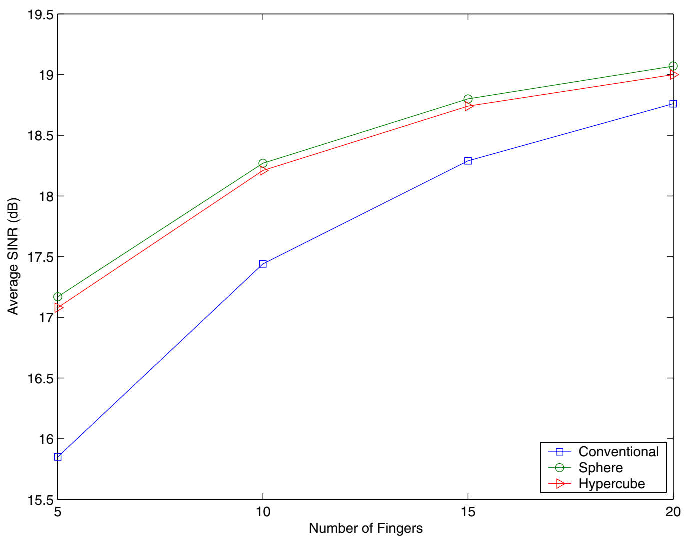

Fig. 4. Average SINR versus number of fingers M, for $E_b/N_0 =$ 20dB, $N_c = 75$ and $L = 50$. All the other parameters are the same as those for Figure 3.

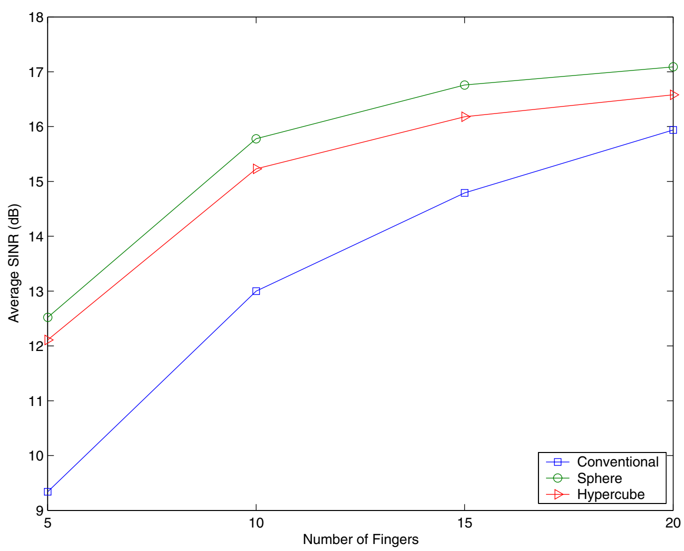

Fig. 5. Average SINR versus number of fingers M. There are 10 users with each interferer having 10dB more power than the desired user. All the other parameters are the same as those for Figure 4.

ered. Since UWB systems have large number of multipath components, only a subset of those components can be used due to complexity constraints. Therefore, the selection of the optimal subset of multipath components is important for the performance of the receiver. We have shown that the optimal solution to this finger selection problem requires exhaustive search which becomes prohibitive for UWB systems. Therefore, we have proposed approximate solutions of the problem based on the Taylor series approximation and integer constraint relaxations. Using two different integer relaxation approaches, we have introduced two convex relaxations of the optimal finger selection algorithm. Implementing these suboptimal algorithms on top of the conventional scheme, we can get close to the optimal solution, with much lower complexity.

The two contributions of the paper are the formulation of the optimal problem and the convex relaxations. In the first, the formulation is globally optimal but the solution methods for non-convex nonlinear integer constrained optimization must use heuristics to get to a locally optimal solution because otherwise computational load for global optimality is too much. In the second, the formulation is relaxed, but the interior-point methods efficiently computes the globally optimal solution for these relaxations.

References

[1] U. S. Federal Communications Commission, FCC 02-48: First Report and Order.

[2] M. Z. Win and R. A. Scholtz, "Impulse radio: How it works," *IEEE Communications Letters,* 2(2): pp. 36-38, Feb. 1998.

[3] M. Z. Win and R. A. Scholtz, "Ultra-wide bandwidth time-hopping spread-spectrum impulse radio for wireless multiple-access communications," *IEEE Transactions on Communications*, vol. 48, pp. 679-691, April 2000.

[4] F. Ramirez Mireless, "On the performence of ultra-wideband signals in gaussian noise and dense multipath," *IEEE Transactions on Vehicular Technology,* 50(1): pp. 244-249, Jan. 2001.

[5] R. A. Scholtz, "Multiple access with time-hopping impulse modulation," *Proc. IEEE Military Communications Conference (MILCOM 1993),* vol. 2, pp. 447-450, Boston, MA, Oct. 1993.

[6] D. Cassioli, M. Z. Win and A. F. Molisch, "The ultra-wide bandwidth indoor channel: from statistical model to simulations," *IEEE Journal on Selected Areas in Communications*, vol. 20, pp. 1247-1257, Aug. 2002.

[7] D. Cassioli, M. Z. Win, F. Vatalaro and A. F. Molisch, "Performance of low-complexity RAKE reception in a realistic UWB channel," *Proc. IEEE International Conference on Communications (ICC 2002),* vol. 2, pp. 763-767, New York, NY, April 28-May 2, 2002.

[8] E. Fishler and H. V. Poor, "On the tradeoff between two types of processing gain," *IEEE Transactions on Communications,* to appear.

[9] S. Gezici, H. Kobayashi, H. V. Poor and A. F. Molisch, "Performance evaluation of impulse radio UWB systems with pulse-based polarity randomization in asynchronous multiuser environments," *Proc. IEEE Wireless Communications and Networking Conference (WCNC 2004),* vol. 2, pp. 908-913, Atlanta, GA, March 2004.

[10] Y.-P. Nakache and A. F. Molisch, "Spectral shape of UWB signals influence of modulation format, multiple access scheme and pulse shape," *Proc. IEEE 57th Vehicular Technology Conference, (VTC 2003-Spring)*, vol. 4, pp. 2510-2514, Jeju, Korea, April 2003.

[11] A. F. Molisch, Y. P. Nakache, P. Orlik, J. Zhang, Y. Wu, S. Gezici, S. Y. Kung, H. Kobayashi, H. V. Poor, Y. G. Li, H. Sheng and A. Haimovich, "An efficient low-cost time-hopping impulse radio for high data rate transmission," *Proc. IEEE 6th International Symposium on Wireless Personal Multimedia Communications (WPMC 2003),* Yokosuka, Kanagawa, Japan, Oct. 19-22, 2003.

[12] S. Gezici, H. Kobayashi, H. V. Poor, and A. F. Molisch, "Optimal and suboptimal linear receivers for time-hopping impulse radio systems," *Proc. IEEE Conference on Ultra Wideband Systems and Technologies (UWBST 2004),* Kyoto, Japan, May 18-21, 2004.

[13] S. Verdú. *Multiuser Detection,* Cambridge University Press, Cambridge, UK, 1998.

[14] S. Boyd and L. Vandenberghe, *Convex Optimization,* Cambridge University Press, Cambridge, UK, 2004.